HHS Public Access

Author manuscript

*Glia*. Author manuscript; available in PMC 2022 June 23.

Published in final edited form as:

*Glia*. 2022 April ; 70(4): 712–727. doi:10.1002/glia.24135.

# Neuronal contact upregulates astrocytic sphingosine-1-phosphate receptor 1 to coordinate astrocyte-neuron cross communication

**Sandeep K. Singh**,

**Tomasz Kordula**,

**Sarah Spiegel**

Department of Biochemistry and Molecular Biology and Massey Cancer Center, Virginia Commonwealth University School of Medicine, Richmond, Virginia, USA

## Abstract

Astrocytes, the most abundant glial cells in the mammalian brain, directly associate with and regulate neuronal processes and synapses and are important regulators of brain development. Yet little is known of the molecular mechanisms that control the establishment of astrocyte morphology and the bi-directional communication between astrocytes and neurons. Here we show that neuronal contact stimulates expression of S1PR1, the receptor for the bioactive sphingolipid metabolite sphingosine-1-phosphate (S1P), on perisynaptic astrocyte processes and that S1PR1 drives astrocyte morphological complexity and morphogenesis. Moreover, the S1P/S1PR1 axis increases neuronal contact-induced expression of astrocyte secreted synaptogenic factors SPARCL1 and thrombospondin 4 that are involved in neural circuit assembly. Our findings have uncovered new functions for astrocytic S1PR1 signaling in regulation of bi-directional astrocyte-neuron crosstalk at the nexus of astrocyte morphogenesis and synaptogenesis.

### Keywords

astrocytes; sphingosine-1-phosphate; synaptogenic factors

## 1 | INTRODUCTION

Astrocytes, the most abundant glial cells in the mammalian brain, are present all across the central nervous system (CNS) and regulate many physiological functions controlling brain homeostasis (Allen & Barres, 2009). Astrocytes provide metabolic support to neurons,

**Correspondence**: Sandeep K. Singh, Department of Biochemistry and Molecular Biology, Virginia Commonwealth University School of Medicine, Richmond, VA 23298, USA. sandeep.singh@vcuhealth.org.

AUTHOR CONTRIBUTIONS

SKS conceived the study; SKS, TK and SS designed the experiments. SKS performed the experiments, analyzed data and arranged the manuscript figures. SKS wrote the paper and TK and SS reviewed and edited the manuscript. SS and TK provided critical reagent support.

CONFLICT OF INTEREST

The authors declare no potential conflict of interest.

SUPPORTING INFORMATION

Additional supporting information may be found in the online version of the article at the publisher's website.

modulate neuronal circuit assembly and functions, establish blood brain barrier integrity, and regulate ion homeostasis (Allen & Barres, 2009). They perform most of these functions by acquiring complex morphologies and directly associating with and regulating neuronal processes including synapses via contact-mediated and secreted soluble factors (Allen & Eroglu, 2017; Khakh & Sofroniew, 2015). Bidirectional communication with neurons maintains astrocyte-synapse association and circuit functions (Durkee & Araque, 2019; Martin et al., 2015). While neuron-derived cues such as cardiotrophin-1, ephrins, sonic-hedgehog, and neurexins induce astrocyte differentiation, heterogeneity, and morphological maturation (Farmer et al., 2016; Freeman, 2010; Stogsdill et al., 2017), astrocytes regulate excitatory synapse formation, function and plasticity by secreted several factors including, SPARCL1 (also known as hevin), thrombospondins (TSP1-4), glypicans, and norrin (Eroglu et al., 2009; Miller et al., 2019; Singh et al., 2016). SPARCL1 induces thalamocortical excitatory synaptogenesis, recruits NMDAR subunits to the postsynapses, and is required for the plasticity of the thalamocortical connections in the developing visual cortex (Singh et al., 2016). Astrocytic TSPs also induce excitatory synaptogenesis and are involved in the development of proper barrel cortex plasiticity (Eroglu et al., 2009). Astrocyte morphological complexity and expression of synaptogenic factors are altered in many neuropathologies including, autism, Alzheimer's disease, schizophrenia, and neuropathic pain (Blanco-Suarez et al., 2017; Burda & Sofroniew, 2014; Ji et al., 2019; Seddighi et al., 2018). However, mechanisms regulating expression of the synaptogenic factors and astrocyte-neuron interactions are yet to be fully explored.

Sphingosine-1-phosphate (S1P), a bioactive metabolite of membrane sphingolipids that are highly enriched in the brain, plays an important role in regulation of neuronal survival, neurite growth, synaptic transmission, myelination, oligodendrocyte development, and neuroinflammation (Bryan et al., 2008; Cartier & Hla, 2019; Karunakaran & van Echten-Deckert, 2017). S1P binds to and activates five specific G protein-coupled receptors (GPCR) named S1PR1-5 (Spiegel & Milstien, 2011). S1PR5 is specifically expressed in oligodendrocytes and regulates their survival and development (Jung et al., 2007). S1PR1 has been associated with reactive astrocytes and neuroinflammation (Choi et al., 2011; Kim et al., 2018; Singh & Spiegel, 2019). Astrocyte specific deletion of S1PR1 protected mice from experimental autoimmune encephalomyelitis (EAE) (Choi et al., 2011), a model for multiple sclerosis (MS), and from development of neuropathic pain (Chen et al., 2019; Stockstill et al., 2018). Furthermore, FTY720 (Fingolimod, Gilenya), primarily a S1PR1 modulator used for treatment of MS, drastically suppresses demyelination, axonal loss, and astrogliosis in EAE (Choi et al., 2011). FTY720 also suppressed chemotherapy induced- and nerve injury derived neuropathic pain (Chen et al., 2019; Stockstill et al., 2018). FTY720 is a pro-drug phosphorylated in vivo to a S1P mimetic that acts as a functional antagonist of S1PR1 suppressing lymphocyte egress from lymphoid organs and thus, limiting CNS attack by pathogenic lymphocytes. Importantly, its efficacy in EAE and neuropathic pain has also been linked to antagonism of astrocytic S1PR1 signaling (Chen et al., 2019; Choi et al., 2011; Singh & Spiegel, 2019; Stockstill et al., 2018).

Although, S1P-S1PR signaling has attracted much attention as a drug target for treatment of MS and other neurological disorders, its roles in regulating astrocyte-neuron interactions during brain development and in neurological disorders are largely unknown. Here,

we examined the involvement of astrocytic S1PRs in bidirectional astrocyte-neuron communication. We discovered that S1PR1 controls astrocyte complexity, astrocyte-neuron interactions, and plays a critical role regulating expression of astrocyte-secreted SPARCL1 and TSP4 proteins that control structural synapse formation and neuronal circuit assembly.

## 2 | MATERIALS AND METHODS

### 2.1 | Mice

*S1pr1*$^{eGFP/eGFP}$ mice (B6.129P2-S1pr1tm1Hrose/J) on C57Bl/6J background were from Jackson Laboratory (Bar Harbor, ME, #028623) and housed in the animal care facilities at Virginia Commonwealth University under standard temperature, humidity, and timed light conditions and provided with standard rodent chow and water ad libitum. The Institutional Animal Care and Use Committee of Virginia Commonwealth University approved all animal protocols and procedures.

### 2.2 | Brain tissue collection

Two pups were randomly collected from the same litter at the indicated postnatal age (between P5 and P21). Brain regions (cortices and cerebella) were dissected out quickly and immediately flash frozen in liquid nitrogen and stored at −80°C. Frozen tissues were crushed into powder using a tissue pulverizer on dry ice and lysed in TRIzol reagent (Invitrogen) to isolate total RNA or in modified RIPA buffer for protein analyses.

### 2.3 | Astrocyte, neuron culture, and coculture

Human cortical astrocytes were prepared from fetal tissue from Advanced Bioscience Resources (Alameda) and cultured in DMEM media supplemented with 10% fetal bovine serum, non-essential amino acids, pen/strep, sodium pyruvate and glutamine as described previously (Kordula et al., 1998). Briefly, human cortical astrocyte cultures were established using dissociated human cerebral tissue at 16–20 week gestation. Cortical tissue was washed with PBS, mechanically dissociated by repeated pipetting, and the solution was passed through a 100 μm nylon cell strainer (Falcon). The cells obtained were pelleted by centrifugation for 5 min at 200× *g*, resuspended in a trypsin/EDTA solution (0.05% trypsin and 0.53 mm EDTA in Hanks' balanced salt solution, Life Technologies, Inc.), and incubated for 20 min at 37°C. Modified Eagle's medium containing 1% glucose, 1 mm sodium pyruvate, 1 mm glutamine, and 10% fetal bovine serum (MEM/FBS) and DNase (final concentration of 0.05 mg/ml) were added, and the cells were pelleted and resuspended in MEM/FBS. $1.6 \times 10^8$ cells were seeded in a T-150 tissue culture flask coated with poly-D-lysine. Cultures were maintained in an $H_2O$-saturated incubator with an atmosphere of 95% air and 5% $CO_2$ at 37°C. The culture medium was changed 1 and 4 days after plating, and the cultures were then left undisturbed for at least 1 week. The cells from one T-150 flask were replated into three to five T-150 flasks. Just before confluence, the cells were re-passaged by trypsinization. The human astrocytes used in this study were >99% pure as determined by GFAP positive cells and lack of Cd11b or CC1 staining (Gupta et al., 2019).

Mouse cortical neurons were isolated by immunopanning as described (Singh et al., 2016). Briefly, cortices were dissected from P1 pups and digested with papain (Worthington Biochemical Corp), followed by low and high concentrations of ovomucoid incubation to inhibit papain. Triturated cells were first passed through 40 μm nitex filters (Fisher Scientific) and then applied to a series of negative panning dishes (to remove unwanted cells and debris): 2× Bandeiraea Simplicifolia Lectin I-coated petri dishes (Vector Laboratories); AffiniPure goat-anti mouse IgG + IgM (H + L) (Jackson Immunoresearch Laboratories, PA) coated dish; and AffiniPure goat-anti rat IgG (H + L) (Jackson) coated dish. Cell suspensions were then incubated with rat anti-neural cell adhesion molecule L1 (MAB5272, Millipore) coated positive panning dishes to obtain >95% pure cortical neurons. Cortical neurons were then plated on poly-d-lysine (PDL) and laminin coated glass coverslips in 24-well plates (for imaging studies) or in 12 well plates (for gene expression analyses) containing neuronal growth medium (NGM) comprised of neurobasal media supplemented with SATO (Gibco), BDNF (Peprotech), CNTF (Peprotech) and forskolin (Sigma). Neurons were cultured in a humidified chamber with 10% CO2 at 37°C. Half of the media was replaced with fresh NGM every 3 days. Additionally, AraC (2 μm) was added for 24–36 h to prevent contaminating glial cell growth.

### 2.4 | Coculture of human astrocytes with mouse cortical neurons and S1P stimulation

Human astrocytes were cultured for 5–6 days in 10% FBS containing DMEM medium, trypsinized, counted, and resuspended in serum-free neuronal growth medium and plated on DIV6-8 cortical neuronal cultures maintained in serum-free neuronal growth medium at a neuron to astrocyte ratio of 3:1 which is similar to the ratio found in human brain cortex (Herculano-Houzel, 2014) and as used by others (Baldwin et al., 2021; Stogsdill et al., 2017). Twelve to sixteen hours later, cocultures were treated with S1P (100 nM) for the indicated times.

### 2.5 | Transfection and knockdown

Human astrocytes were transfected with pEYFP-C1 plasmid from Clontech (Mountain View, CA) using Lipofectamine 2000 plus (Life Technologies). Twenty to twenty-four hours later, transfected astrocytes were trypsinized, counted, resuspended in NGM and plated on neuronal cultures at a neuron to astrocyte ratio of 3:1. For downregulation, human astrocytes were transfected with 50 nM SmartPool siRNAs (#L-003655-00-0005) using Lipofectamine 2000 plus (Life Technologies), according to the manufacturer's instructions. Thirty-six to forty hours after siRNA transfection, astrocytes were trypsinized, counted and plated on neuronal cultures at a neuron to astrocyte ratio of 3:1.

### 2.6 | RNA isolation and quantitative PCR

Total RNA was prepared from flash frozen tissue or cells with Trizol (Life Technologies). RNA was treated with DNAse (Promega), then reverse transcribed with a high-capacity cDNA kit (Applied Biosystems) and amplified on the BioRadCFXConnect Real-time System. Species (human or mouse) and gene specific pre-designed SYBR green primers (Bio-Rad) were used. Gene expression levels were normalized to either 18S RNA or GAPDH and presented as fold expression over the control.

### 2.7 | Western blotting

Powdered brain tissue was lysed in ice-cold modified RIPA buffer (20 mM Tris pH 7.4, 150 mM NaCl, 1 mM $CaCl_2$, 1 mM $MgCl_2$, 1% Triton-X100, 0.5% NP-40 and protease/phosphatase inhibitor). After sonication, supernatants were collected after centrifugation at 12,000 rpm for 15 min at 4°C. Proteins were quantified by BCA protein assay kit (Pierce; #23227), and equal amounts were separated by SDS-PAGE on precast gradient gels (Bio-Rad) and transferred onto nitrocellulose membranes (Bio-Rad). Blots were first blocked in 10% blotting grade milk and then incubated with the following primary antibodies: anti-β-tubulin (1:2000) (Santa Cruz Biotechnology; sc-9104), anti-S1PR1 (1:1000) (Millipore; MABC94), anti-GFAP (1:1000) (Cell Signaling; #3670), and anti-SPARCL1 (1 μg/ml) (Singh et al., 2016). Immunopositive bands were visualized on X-ray films by chemiluminescence with horseradish peroxide conjugated secondary antibodies (anti-rabbit #111035045 or anti-mouse #115035166 or anti-rat #112035003 (Jackson ImmunoResearch Laboratories, West Grove, PA, USA) and Pico Plus substrate (Thermo Fisher Scientific). ImageJ was used to quantify band intensities of respective blots from scanned images of X-ray films. Tubulin band intensity was used to normalize the expression levels.

### 2.8 | Immunofluorescence

*S1pr1*$^{eGFP/eGFP}$ mice were perfused intracardially with Tris-buffered saline (TBS, 25 mM Tris-base, 135 mM NaCl, 3 mM KCl, pH 7.6) supplemented with 7.5 μM heparin followed with 4% paraformaldehyde (PFA; Electron Microscopy Sciences, PA) in TBS. Brains were removed and fixed for 24 h in 4% PFA and then cryopreserved in 30% sucrose (in 1μ TBS) for 2–3 days at 4°C. Sucrose immersed brains then were embedded in 2:1 mixture of 30% sucrose/OCT medium. Twenty-five micrometers of sagittal sections were prepared using a cryostat (Thermo) and stored as floating sections in 1:1 glycerol/TBS solutions in −20°C (Risher et al., 2014). Sections were washed three times in TBS, then blocked with 10% normal goat serum and 0.2% Triton-X100 in TBS for 1 h at room temperature. Sections were incubated overnight at 4°C with the following antibodies in blocking buffer: anti-GFAP (1:500, Cell Signaling; #3670), anti-MAP2 (1:500, Cell Signaling; #8707), anti-GLT1 (1:400, Millipore; AB1783), anti-calbindin (1:1000, Cell Signaling; #13176), and anti-SPARCL1 (1 μg/ml). Subsequently, sections were washed and incubated with species-specific secondary antibodies conjugated with Alexa Fluor 594 or Alexa Flour 647 (1:1000 or 1:500, respectively, Invitrogen) for 2 h at room temperature, followed by washing with TBS and finally mounted with DAPI containing Vectashield mounting media (Vector labs). Sections were imaged using Zeiss LSM 880, Zeiss LSM 710, BZ-X810 (Keyence) or ZOE fluorescent imager (Bio-rad) as indicated. Tiled images in Zeiss 880 were obtained using a 10X magnification lens with a 15% overlap between tiles. Confocal images were taken with 1 μm step sizes in 5–8 Z-stacks comprising a total of 5–8 μm. Representative images were processed for average intensity projections of 1–2 optical steps in FIJI. Three to six images were acquired per animal.

### 2.9 | Image analyses

For assays of astrocyte morphological complexity, eYFP+ astrocyte signals were imaged randomly at 20X in each condition. Complexity was analyzed by Sholl analyses plugin in FIJI. SPARCL1 signal intensity was quantified by determining the integrated signal intensity of SPARCL1 in red per image. Briefly, the red channel was first converted into a gray scale image, followed by an image color threshold step. Then integrated signal intensity was quantified with the analyze measure tool. Perimeter of astrocytes were determined as the overall periphery of GFAP stained areas in FIJI using the analyze measure tool after the images were converted into a binary profile. An example image with its perimeter tracing as obtained from FIJI is found in Figure S5.

### 2.10 | Statistical analyses

Statistical significance was determined by unpaired 2-tailed Student t tests for comparison of 2 groups or ANOVA with post hoc analysis for multiple groups (GraphPad Prism 9). $p \leq .05$ was considered significant. The number of independent experiments ($n$) and the number of analyzed cells is noted in figure legends. All biochemical data were from biological triplicates, whereas imaging data was quantified from multiple cells as indicated in the figure legends.

## 3 | RESULTS

### 3.1 | Increased expression of S1PR1 during postnatal mouse brain development

Although S1P-S1PR signaling has been extensively studied in several neuropathological states and in cultured CNS cells, not much is known on their functions in developing brain. We examined the mRNA expression of S1PRs as assessed by qPCR in the developing mouse cortex and cerebellum during postnatal days 5–21 (P5-P21), when astrocyte morphogenesis occurs concomitantly with synaptic development (Morel et al., 2014). Expression of S1PR1 and S1PR5 gradually increased between postnatal day P5 and P21 in both cortex and cerebellum (Figure 1a,b). The increase in S1PR5 expression is consistent with previous report that S1PR5 is expressed by oligodendrocytes (Terai et al., 2003), which are responsible for myelination that occurs during the early postnatal development. In contrast to S1PR1 and S1PR5, there were no major changes in the expression of S1PR2 and S1PR3, while S1PR4 significantly increased only in the cortical tissue (Figure 1a,b).

Because the first 3 weeks of postnatal mouse brain development is associated with synaptogenesis, circuit formation, and astrocyte maturation, we examined expression of astrocyte-secreted synaptogenic factors SPARCL1 and TSPs. As expected, expression of SPARCL1 and TSP4 also gradually increased during this period in the cortex (Figure 1a) as previously reported (Christopherson et al., 2005; Risher et al., 2014). While SPARCL1 expression increased in the cerebellum, TSP4 expression decreased (Figure 1a,b), suggesting brain region specific expression of TSP4. In addition, expression of the other TSPs was relatively unchanged except that TSP1 expression significantly decreased only in the cortex (Figure 1a,b). Western blot analysis confirmed increased expression of S1PR1 and SPARCL1 in cortical and cerebellar tissue (Figure 1c,d, Figure S1). As expected,

expression of a well-known astrocyte marker, glial fibrillary acidic protein (GFAP), was also upregulated during the development of the CNS.

To further explore the expression of S1PR1 in mouse brain, we utilized S1PR1 reporter mice (*S1pr1*$^{eGFP/eGFP}$) in which the EGFP gene is inserted downstream of the coding region of the *S1pr1* gene allowing the monitoring of S1PR1 protein expression at cell-type and tissue levels (Cahalan et al., 2011). Confocal analysis showed S1PR1-eGFP signals in all brain regions including cortex, hippocampus, and cerebellum (Figure 2a,b). Consistent with mRNA expression (Figure 1a,b), S1PR1 protein also increased from P8 to P21. S1PR1 was highly expressed in the cerebellum, particularly in the area corresponding to the molecular layer (ML), which harbors Purkinje cell (PC) dendrites and Bergman glia (BG) processes. Moreover, there was no detectable GFP signal in the corpus callosum (CC) or white matter (WM) of the cerebellum (Figure 2a,b). Consistent with the S1PR1-eGFP fluorescence (Figure 2a,b), the in situ expression data (the Allen-Brain Atlas (http://atlas.brain-map.org) confirmed a widespread expression of S1PR1 throughout the brain, with high expression levels in the cerebellar molecular layer (Figure 2c). These findings suggest that S1PR1 expression coincides with the developmental phase of synaptogenesis and astrocyte maturation in the rodent brain.

### 3.2 | S1PR1 is primarily expressed on peripheral processes of astrocytes

To further characterize expression of S1PR1 in CNS cells, we first analyzed its expression in publicly available databases (www.brainrnaseq.org). In both mouse and human brain, the highest expression levels of S1PR1 were found in astrocytes and were even greater than in brain endothelial cells known to express high levels of S1PR1 (Figure 3a). In comparison, neurons, oligodendrocytes, and microglia expressed S1PR1 at very low levels (Figure 3a). Interestingly, there was a 50-fold increase in S1PR1 expression in mature human astrocytes compared to fetal astrocytes, suggesting a critical role of S1PR1 in the mature cells (Figure 3a). We further sought to corroborate S1PR1 mRNA abundance by characterizing S1PR1 protein expression in S1PR1-eGFP knock-in mouse brain. The S1PR1-eGFP mouse brain sections were immunostained for astrocyte marker GFAP and neuronal dendrite marker MAP2 and visualized by confocal microscopy (Figure 3b,c). As expected, GFAP staining was almost completely absent in the cortical area but abundant in the hippocampus and cerebellum (Figure 3b). However, only a small proportion of S1PR1-eGFP signal colocalized with GFAP in the hippocampus and in the cerebellar molecular layer (ML) (arrows) (Figure 3b). Since, S1PR1 is a GPCR primarily located on the plasma membrane, as expected, it did not extensively colocalize with intracellular cytoskeletal protein GFAP. There was also no co-localization of eGFP signal with neuronal MAP2 (Figure 3c).

Astrocytes acquire complex morphologies generating thousands of fine peripheral astrocyte processes or perisynaptic astrocyte processes (PAPs) during their maturation (Heller & Rusakov, 2015). PAPs are found near and around synapses and are marked by the presence of glutamate transporter 1 (EAAT2 or GLT1) and water channel aquaporin 4 (AQP4). Interestingly, we found that S1PR1-eGFP signal strongly colocalized with both GLT1 and AQP4 in the cortex, hippocampus, and cerebellum (Figure 4a,b). It is also noteworthy that

not all S1PR1-eGFP was associated with GLT1 and AQP4 staining. Taken together, these data demonstrate that S1PR1 is primarily expressed by astrocytes and is predominantly present on PAPs.

### 3.3 | S1PR1 is highly expressed by the Bergman glia of the cerebellum

Because PAPs are generated during astrocyte maturation (Farmer et al., 2016; Tsai et al., 2012), we investigated changes in expression of S1PR1 in the developing molecular layer of cerebella during postnatal days 8–21, when astrocytes mature concomitantly with the development of synapses (Farmer et al., 2016; Heller & Rusakov, 2015). Cerebellar S1PR1-eGFP sections were immunostained for SPARCL1, an astrocytic protein specifically required for the formation of a subset of excitatory synapses (Singh et al., 2016) and for Purkinje cell (PC) marker calbindin. Although S1PR1-eGFP signal was found in both the granule cell layer and ML, it was most abundant in the ML (Figure 5a). Structurally, ML is primarily comprised of three components: synapse dense PC dendrites; BG-main radial processes spanning the ML; and BG-fine peripheral processes ensheathing PC synapses (Cerminara et al., 2015). S1PR1-eGFP did not colocalize with calbindin stained PC neuronal processes (Figure 5c) but was present on the main and peripheral processes of BG expressing SPARCL1 (arrows) (Figure 5a,b). Moreover, S1PR1-eGFP on BG peripheral processes extended over only half of the ML at P8 but over the entire ML by P21 (Figure 5a,b). As this BG-peripheral process growth pattern coincided with PC dendritic growth during this developmental period (Lordkipanidze & Dunaevsky, 2005), our findings suggest that S1PR1 expression may regulate cross-communication of BG and PC during development.

### 3.4 | Neuronal contact stimulates S1PR1 expression in astrocytes

Interaction of PAPs with dendritic spines is highly dynamic and modulates synaptic function (Heller & Rusakov, 2015). In turn, neuronal contact stimulates astrocyte morphological complexity, PAP growth, and PAP-synapse association (Stogsdill et al., 2017). Because S1PR1 is present on PAPs and is thus poised to regulate neuron-astrocyte interaction, we further explored the role and regulation of S1PR1 expression in astrocyte-neuron cross-communication. To this end, we developed an in vitro coculture of mouse cortical neurons with human astrocytes. This unique coculture system enabled us to analyze changes in gene expression in both astrocytes and neurons (Figure 6a). Astrocytic expression can be selectively measured due to the human specific qPCR primers (Figure S2). Surprisingly, co-culture with neurons induced 3.5-fold induction in the expression of astrocyte S1PR1 compared to the astrocyte alone cultures (Figure 6b). In contrast, expression of other S1PRs present on astrocytes, S1PR2, S1PR3, and S1PR5, was significantly decreased in the cocultures (Figure 6b). Because S1PR1 expression coincides with the expression of SPARCL1 and TSP4 in the developing brain (Figure 1), we next analyzed expression of these synaptogenic factors in the in vitro cocultures. Similarly, to S1PR1 expression pattern, expression of both SPARCL1 and TSP4 increased in astrocytes when cocultured with neurons (Figure 6c). We also measured the expression of gene products expressed by matured astrocytes including, GFAP, nuclear factor I X (NFIX), glial high-affinity glutamate transporter (GLAST), and glutamate transporter 1 (GLT1). While expression of NFIX was increased, GFAP levels decreased and GLT1 and GLAST remained unaltered (Figure

6c), suggesting that coculture with neurons does not induce maturation of astrocytes but specifically upregulates expression of synaptogenic factors and that astrocytes may become receptive to S1P signaling primarily via S1PR1 signaling.

### 3.5 | Neuronal contact dependent expression of synaptogenic SPARCL1 and TSP4 in astrocytes is induced by S1P/S1PR1 axis

As astrocytic S1PR1, SPARCL1 and TSP4 expression was induced by neuronal contact, we asked whether the S1P/S1PR1 axis regulates expression of these synaptogenic factors. Astrocytes alone or cocultured with neurons were stimulated with S1P, the natural ligand for S1PR1. Interestingly, S1P stimulated expression of both SPARCL1 and TSP4 only in astrocytes cocultured with neurons but had little or no effect on astrocytes alone (Figure 7a). This response was rapid with expression of SPARCL1 and TSP4 peaking at 2 h and 8 h respectively (Figure 7a). The observed induction was very specific as no changes in expression of the two other TSP family genes TSP1 and TSP2 were noted (Figure 7a). To further demonstrate the critical role of S1PR1, its levels were downregulated in astrocytes using specific S1PR1 siRNA (siS1PR1) prior to coculture with neurons. Expression of S1PR1 was efficiently downregulated by more than 70% (Figure 8a). We have verified that transfection did not affect the reactivity status of astrocytes by measuring mRNA expression of reactive astrocyte marker genes including SERPINA3N, TIMP1, S100b, and GFAP (Figure S3) (Escartin et al., 2021; Liddelow et al., 2017). Significantly, S1P-stimulated expression of both SPARCL1 and TSP4 in astrocytes co-cultured with neurons was completely blocked by S1PR1 siRNA but not by control siRNA (Figure 8a). In contrast, downregulation of S1PR1 did not alter expression of other gene products expressed by astrocytes, including S1PR3, TSP1, NFIX, and GLAST (Figure 8b). Furthermore, silencing S1PR1 also reduced SPARCL1 immunostaining specifically in astrocytes contacting neurons (Figure 8c). Taken together, these data suggest that the S1P/S1PR1 axis is critical for neuronal contact-induced expression of astrocyte synaptogenic factors SPARCL1 and TSP4.

### 3.6 | Neuronal contact-induced morphological complexity of astrocytes depends on S1PR1

Because S1PR1 is expressed on PAPs (Figure 4) and is also associated with the arborization of BG peripheral processes (Figure 5), we wondered whether astrocyte S1PR1 might control astrocyte morphological complexity. Consistent with previous studies (Hasel et al., 2017; Stogsdill et al., 2017), astrocyte complexity, determined by Sholl analyses as the number of intersections at a given periphery, was greatly enhanced by coculture with neurons with longer and increased branching compared to astrocytic monocultures (Figure 9a,b). The increased complexity was also corroborated by the increased perimeter of astrocytes in cocultures (Figure 9c). Interestingly, we also observed that human astrocytes when cultured in the absence of neurons showed larger cell soma (Figure 9a,b). We speculate that neuronal presence drives astrocytic morphological changes such that astrocytic soma size is reduced and membrane is utilized to create extended complex branching with finer processes ready to contact and ensheath synapses. In an in vivo setting, this might also ensure that most of the neuropil is available for formation of synaptic connections and their association with astrocyte fine processes but not occupied by astrocytic large soma. Indeed, in the developing mouse visual cortex, astrocyte cell soma appears larger at

postnatal day P7 (when neuronal connections have not established yet and astrocytes are morphologically less complex) compared to that at P21 (when neuronal connections have established, and astrocytes have acquired complex morphology) (Stogsdill et al., 2017). To directly demonstrate the significance of S1PR1 signaling in astrocyte morphological complexity, we used the S1PR1 antagonist W146 (Gonzalez-Cabrera et al., 2008) and siRNA approaches. Treatment with W146 (Figure 9d) or downregulation of S1PR1 (Figure 9e) significantly altered complexity of the co-cultured astrocytes, which were characterized by shorter processes, fewer branches, and decreased perimeters (Figure 9a–e). To further validate the direct effect of S1P on astrocyte complexity, human astrocyte and mouse neuronal cocultures were treated with 100 nM S1P for 21 h. S1P potently induced astrocytic morphological complexity determined by Sholl analyses (Figure S4). Next, we tested whether S1PR1 also controls astrocyte-synapse association. We downregulated S1PR1 in astrocytes and cocultured with neurons and stained for postsynaptic marker protein homer-1 (Figure 9f,g). Interestingly, homer-1 puncta associated with astrocytic processes were significantly reduced by S1PR1 downregulation (Figure 9f,g), while the size of the homer-1 puncta remained unchanged (Figure 9, right panel). These data suggest that S1PR1 signaling in astrocytes is needed for neuronal contact-induced growth of astrocyte processes, generation of astrocyte complexity, and astrocyte-synapse association.

## 4 | DISCUSSION

Although astrocytes were initially considered as non-excitable and space filling cells in the brain, these cells have emerged as key players actively regulating neuronal synaptic circuit assembly and functions as well as animal behavior (Stogsdill & Eroglu, 2017). Astrocytes contact the majority of synapses by their PAPs and modulate synapse formation and synaptic transmission by releasing soluble synaptogenic signals such as SPARCL1 and TSPs, gliotransmitters D-serine and ATP, and by maintaining ion homeostasis in the extrasynaptic milieu (Stogsdill & Eroglu, 2017). Emerging evidence indicates the existence of dynamic interplay between astrocytes and neurons beyond the tight physical and functional association between neuronal synapses and PAPs (Allen & Eroglu, 2017; Bernardinelli et al., 2014; Lavialle et al., 2011). However, the mechanisms regulating these dynamic interactions have just begun to be explored. In this work, we show that neuronal contacts induce expression of S1PR1 in astrocytes and stimulation of S1PR1 in turn regulates expression of astrocyte synaptogenic factors SPARCL1 and TSP4. Moreover, S1PR1 is expressed on PAPs and its expression is developmentally regulated in rodent brain.

Previously we showed that SPARCL1 secreted by astrocytes recruits NMDARs at the postsynapse, induces vesicular glutamate transporter 2 (VGLUT2) positive thalamocortical synapse formation, and plasticity in the developing visual cortex (Singh et al., 2016). Expression of SPARCL1 is upregulated during astrocyte differentiation by DNA demethylation of its promoter and binding of the transcription factor NFIX (Hatada et al., 2008; Singh et al., 2011; Wilczynska et al., 2009). However, the signals that regulate expression of SPARCL1 were unknown. After an extensive screening of many bioactive molecules, including cytokines, growth factors, and numerous lipids (data not shown), we discovered that S1P specifically induced SPARCL1 expression in astrocytes cocultured with neurons by binding to S1PR1. In our knowledge this is the first evidence that

an external signal stimulate expression of SPARCL1 in astrocytes. Since we found that downregulation of S1PR1 in astrocytes cocultured with neurons does not significantly alter NFIX expression, this transcription factor is not likely regulating SPARCL1 expression in response to S1PR1 activation. S1P-S1PR1 signaling has been reported to activate STAT3 (Lee et al., 2010; Liang et al., 2013), which is an established astrocyte differentiation factor (Bonni et al., 1997). Thus, it is tempting to speculate that STAT3 could contribute to regulation of SPARCL1 expression.

Like SPARCL1, TSPs have also been shown to induce excitatory synapse formation in cultured neurons (Eroglu et al., 2009). Furthermore, TSP4 contributes to neuropathic pain generation by increasing VGLUT2 positive synapses and their activity in the dorsal horn of the spinal cord (Park et al., 2016). Because the kinetics of TSP4 and SPARCL1 induction by S1P/S1PR1 were dissimilar, it is likely that distinct downstream pathways are involved. Furthermore, developmental changes in expression of TSP4 are similar to the changes of SPARCL1 and S1PR1 expression in the cortex, but not in the cerebellum. Since astrocytes are heterogeneous and exhibit distinct expression and functional profiles to accordance with local needs (Huang et al., 2020), different population of astrocytes may also differentially regulate expression of SPARCL1 and TSP4 in response to S1P/S1PR1 signaling.

S1PR1 expression gradually increases in developing mouse brains and neuronal contact stimulates expression of S1PR1 in astrocyte cocultures, suggesting a continuous cell-cell interaction-based mechanism may increase S1PR1 expression. It was reported that neurons synthesize and secrete the neurotrophic cytokines that activate the gp130-JAK-STAT3 signaling pathway important for astrocyte development in vitro (Barnabe-Heider et al., 2005). As STAT3 transcriptionally upregulate S1PR1 expression (Lee et al., 2010; Liang et al., 2013), it is possible that JAK-STAT signaling also drives neuronal contact-mediated S1PR1 expression in astrocytes. We have uncovered new functions for astrocytic S1PR1 signaling in regulation of bi-directional astrocyte-neuron crosstalk that controls astrocyte complexity and morphogenesis and astrocyte-synapse association. Astrocytic S1PR1 might also regulate synapse formation and function by increasing the expression of synaptogenic factors, such as SPARCL1 and TSP4. PAPs are highly dynamic structures, particularly in the developing brain as well as during synaptic activity, regulated by Rho/Rac/cdc42 GTPases (Kofuji & Araque, 2021). Activation of Rac1 or CDC42 enhances PAPs formation. Because, S1PR1 is primarily localized to the PAPs and S1P-S1PR1 signaling activates these GTPases (Toman et al., 2004), S1PR1 may regulate astrocyte morphogenesis via Rac1- and CDC42-mediated actin rearrangements. S1PR1 is predominantly coupled to Gi. Studies using Designer Receptors Exclusively Activated by Designer Drugs (DREADD)-based chemogenetic tools showed that astroglial activation by $G_{i/o}$ protein-mediated signaling stimulated gliotransmitter release, which increased neuronal excitability (Durkee et al., 2019). Moreover, long term Gi-DREADD but not Gq-DREADD activation specifically in visual cortical astrocytes was required for proper visual circuit plasticity (Hennes et al., 2020). Similarly, Gi-DREADD activation in hypothalamic astrocytes modulated hypothalamic neural circuit function and ghrelin-dependent food intake (Yang et al., 2015). Thus, S1PR1 present on the PAPs are poised to regulate Gi-dependent astrocyte-neuron interplay and modulate circuit functions. These could be either by modulation of short-

term Ca2+-regulated gliotransmitter release or long-term modulation of gene expression of synaptogenic factors, such as SPARCL1 and TSP4.

Since S1P levels increase during the first 4 weeks of cortical development in rodents (Davis et al., 2020), S1P-S1PR1 signaling may be crucial for the proper development of neural circuits and their functions. S1P can be generated by neurons, astrocytes and microglia during neuronal activity or neuroinflammation (Anelli et al., 2005; Karunakaran & van Echten-Deckert, 2017). Because S1PR1-5 are differentially expressed in these cells, S1P-S1PR signaling in cocultures could imply a complex system of paracrine or autocrine regulation (Karunakaran & van Echten-Deckert, 2017). Indeed, S1P activation of S1PR2 in cultured astrocytes increases mitochondrial oxygen consumption and inhibits excess extracellular glutamate uptake, which could contribute to neurotoxicity (Jonnalagadda et al., 2021). S1P has been shown to regulate presynaptic release of glutamate and it is also known that synaptic depolarization induces S1P release near vesicular release sites at the plasma membrane (Kajimoto et al., 2007). These observations suggest that S1P might be released at the neuronal presynaptic terminal during synaptic activity. Interestingly, levels of S1P, S1PR1, SPARCL1, and TSP4 are altered in many synaptopathology-associated disorders including, AD and neuropathic pain (Wang & Bieberich, 2018) (Pan et al., 2016; Seddighi et al., 2018; Singh & Spiegel, 2019). Thus, our current findings placing the S1P/S1PR1 axis as critical regulator of both astrocyte morphogenesis and astrocyte-neuron crosstalk, could have important implication not only for brain development but also for these neurological disorders.

## Supplementary Material

Refer to Web version on PubMed Central for supplementary material.

## ACKNOWLEDGMENTS

This work was supported by a NARSAD Young Investigator Grant from the Brain and Behavior Research Foundation to S.K.S. and Massey Cancer Center support grant P30 CA106059 to S.K.S. and R01 GM043880 to S.S. T.K. is supported by R21NS118359. Microscopy was performed at the VCU Microscopy Facility, supported, in part, by funding from NIH-NCI Cancer Center Support Grant P30 CA016059.

### Funding information

Brain and Behavior Research Foundation, Grant/Award Number: NARSAD Young Investigator Award; Massey Cancer Center support grant, Grant/Award Number: P30 CA106059; NIH-NIGMS, Grant/Award Number: R01GM043880; NIH-NINDS, Grant/Award Number: R21NS118359; NIH-NCI Cancer Center, Grant/Award Number: R01AI125433

## DATA AVAILABILITY STATEMENT

The data that support the findings of this study are available from the corresponding author upon reasonable request.

## Abbreviations:

| | |
|---|---|
| **MS** | multiple sclerosis |
| **S1P** | sphingosine-1-phosphate |

| | |
|---|---|
| **SPARCL1** | secreted protein acidic rich in cysteine like 1 |
| **TSP** | thrombospondin |

## REFERENCES


Allen NJ, & Barres BA (2009). Neuroscience: Glia–more than just brain glue. Nature, 457(7230), 675–677. 10.1038/457675a [PubMed: 19194443]

Allen NJ, & Eroglu C (2017). Cell biology of astrocyte-synapse interactions. Neuron, 96(3), 697–708. 10.1016/j.neuron.2017.09.056 [PubMed: 29096081]

Anelli V, Bassi R, Tettamanti G, Viani P, & Riboni L (2005). Extracellular release of newly synthesized sphingosine-1-phosphate by cerebellar granule cells and astrocytes. Journal of Neurochemistry, 92(5), 1204–1215. 10.1111/j.1471-4159.2004.02955.x [PubMed: 15715670]

Baldwin KT, Tan CX, Strader ST, Jiang C, Savage JT, Elorza-Vidal X, Contreras X, Rulicke T, Hippenmeyer S, Estevez R, Ji RR, & Eroglu C (2021). HepaCAM controls astrocyte self-organization and coupling. Neuron, 109(15), 2427–2442e2410. 10.1016/j.neuron.2021.05.025 [PubMed: 34171291]

Barnabe-Heider F, Wasylnka JA, Fernandes KJ, Porsche C, Sendtner M, Kaplan DR, & Miller FD (2005). Evidence that embryonic neurons regulate the onset of cortical gliogenesis via cardiotrophin-1. Neuron, 48(2), 253–265. 10.1016/j.neuron.2005.08.037 [PubMed: 16242406]

Bernardinelli Y, Randall J, Janett E, Nikonenko I, Konig S, Jones EV, Flores CE, Murai KK, Bochet CG, Holtmaat A, & Muller D (2014). Activity-dependent structural plasticity of perisynaptic astrocytic domains promotes excitatory synapse stability. Current Biology, 24(15), 1679–1688. 10.1016/j.cub.2014.06.025 [PubMed: 25042585]

Blanco-Suarez E, Caldwell AL, & Allen NJ (2017). Role of astrocyte-synapse interactions in CNS disorders. The Journal of Physiology, 595(6), 1903–1916. 10.1113/JP270988 [PubMed: 27381164]

Bonni A, Sun Y, Nadal-Vicens M, Bhatt A, Frank DA, Rozovsky I, Stahl N, Yancopoulos GD, & Greenberg ME (1997). Regulation of gliogenesis in the central nervous system by the JAK-STAT signaling pathway. Science, 278(5337), 477–483. 10.1126/science.278.5337.477 [PubMed: 9334309]

Bryan L, Kordula T, Spiegel S, & Milstien S (2008). Regulation and functions of sphingosine kinases in the brain. Biochimica et Biophysica Acta, 1781, 459–466. [PubMed: 18485923]

Burda JE, & Sofroniew MV (2014). Reactive gliosis and the multicellular response to CNS damage and disease. Neuron, 81(2), 229–248. 10.1016/j.neuron.2013.12.034 [PubMed: 24462092]

Cahalan SM, Gonzalez-Cabrera PJ, Sarkisyan G, Nguyen N, Schaeffer MT, Huang L, Yeager A, Clemons B, Scott F, & Rosen H (2011). Actions of a picomolar short-acting S1P(1) agonist in S1P(1)-eGFP knock-in mice. Nature Chemical Biology, 7(5), 254–256. 10.1038/nchembio.547 [PubMed: 21445057]

Cartier A, & Hla T (2019). Sphingosine 1-phosphate: Lipid signaling in pathology and therapy. Science, 366(6463), eaar5551. 10.1126/science.aar5551 [PubMed: 31624181]

Cerminara NL, Lang EJ, Sillitoe RV, & Apps R (2015). Redefining the cerebellar cortex as an assembly of non-uniform Purkinje cell microcircuits. Nature Reviews. Neuroscience, 16(2), 79–93. 10.1038/nrn3886 [PubMed: 25601779]

Chen Z, Doyle TM, Luongo L, Largent-Milnes TM, Giancotti LA, Kolar G, Squillace S, Boccella S, Walker JK, Pendleton A, Spiegel S, Neumann WL, Vanderah TW, & Salvemini D (2019). Sphingosine-1-phosphate receptor 1 activation in astrocytes contributes to neuropathic pain. Proceedings of the National Academy of Sciences of the United States of America, 116(21), 10557–10562. 10.1073/pnas.1820466116 [PubMed: 31068460]

Choi JW, Gardell SE, Herr DR, Rivera R, Lee CW, Noguchi K, Teo ST, Yung YC, Lu M, Kennedy G, & Chun J (2011). FTY720 (fingolimod) efficacy in an animal model of multiple sclerosis requires astrocyte sphingosine 1-phosphate receptor 1 (S1P1) modulation. Proceedings. National Academy of Sciences. United States of America, 108(2), 751–756. 10.1073/pnas.1014154108

Christopherson KS, Ullian EM, Stokes CC, Mullowney CE, Hell JW, Agah A, Lawler J, Mosher DF, Bornstein P, & Barres BA (2005). Thrombospondins are astrocyte-secreted proteins that promote CNS synaptogenesis. Cell, 120(3), 421–433. 10.1016/j.cell.2004.12.020 [PubMed: 15707899]

Davis DL, Mahawar U, Pope VS, Allegood J, Sato-Bigbee C, & Wattenberg BW (2020). Dynamics of sphingolipids and the serine palmitoyltransferase complex in rat oligodendrocytes during myelination. Journal of Lipid Research, 61(4), 505–522. 10.1194/jlr.RA120000627 [PubMed: 32041816]

Durkee CA, & Araque A (2019). Diversity and specificity of astrocyte-neuron communication. Neuroscience, 396, 73–78. 10.1016/j.neuroscience.2018.11.010 [PubMed: 30458223]

Durkee CA, Covelo A, Lines J, Kofuji P, Aguilar J, & Araque A (2019). Gi/o protein-coupled receptors inhibit neurons but activate astrocytes and stimulate gliotransmission. Glia, 67(6), 1076–1093. 10.1002/glia.23589 [PubMed: 30801845]

Eroglu C, Allen NJ, Susman MW, O'Rourke NA, Park CY, Ozkan E, Chakraborty C, Mulinyawe SB, Annis DS, Huberman AD, Green EM, Lawler J, Dolmetsch R, Garcia KC, Smith SJ, Luo ZD, Rosenthal A, Mosher DF, & Barres BA (2009). Gabapentin receptor alpha2delta-1 is a neuronal thrombospondin receptor responsible for excitatory CNS synaptogenesis. Cell, 139(2), 380–392. 10.1016/j.cell.2009.09.025 [PubMed: 19818485]

Escartin C, Galea E, Lakatos A, O'Callaghan JP, Petzold GC, Serrano-Pozo A, Steinhauser C, Volterra A, Carmignoto G, Agarwal A, Allen NJ, Araque A, Barbeito L, Barzilai A, Bergles DE, Bonvento G, Butt AM, Chen WT, Cohen-Salmon M, … Verkhratsky A (2021). Reactive astrocyte nomenclature, definitions, and future directions. Nature Neuroscience, 24(3), 312–325. 10.1038/s41593-020-00783-4 [PubMed: 33589835]

Farmer WT, Abrahamsson T, Chierzi S, Lui C, Zaelzer C, Jones EV, Bally BP, Chen GG, Theroux JF, Peng J, Bourque CW, Charron F, Ernst C, Sjostrom PJ, & Murai KK (2016). Neurons diversify astrocytes in the adult brain through sonic hedgehog signaling. Science, 351(6275), 849–854. 10.1126/science.aab3103 [PubMed: 26912893]

Freeman MR (2010). Specification and morphogenesis of astrocytes. Science, 330(6005), 774–778. 10.1126/science.1190928 [PubMed: 21051628]

Gonzalez-Cabrera PJ, Jo E, Sanna MG, Brown S, Leaf N, Marsolais D, Schaeffer MT, Chapman J, Cameron M, Guerrero M, Roberts E, & Rosen H (2008). Full pharmacological efficacy of a novel S1P1 agonist that does not require S1P-like headgroup interactions. Molecular Pharmacology, 74(5), 1308–1318. 10.1124/mol.108.049783 [PubMed: 18708635]

Gupta AS, Waters MR, Biswas DD, Brown LN, Surace MJ, Floros C, Siebenlist U, & Kordula T (2019). RelB controls adaptive responses of astrocytes during sterile inflammation. Glia, 67(8), 1449–1461. 10.1002/glia.23619 [PubMed: 30957303]

Hasel P, Dando O, Jiwaji Z, Baxter P, Todd AC, Heron S, Markus NM, McQueen J, Hampton DW, Torvell M, Tiwari SS, McKay S, Eraso-Pichot A, Zorzano A, Masgrau R, Galea E, Chandran S, Wyllie DJA, Simpson TI, & Hardingham GE (2017). Neurons and neuronal activity control gene expression in astrocytes to regulate their development and metabolism. Nature Communications, 8, 15132. 10.1038/ncomms15132

Hatada I, Namihira M, Morita S, Kimura M, Horii T, & Nakashima K (2008). Astrocyte-specific genes are generally demethylated in neural precursor cells prior to astrocytic differentiation. PLoS One, 3(9), e3189. 10.1371/journal.pone.0003189 [PubMed: 18784832]

Heller JP, & Rusakov DA (2015). Morphological plasticity of astroglia: Understanding synaptic microenvironment. Glia, 63(12), 2133–2151. 10.1002/glia.22821 [PubMed: 25782611]

Hennes M, Lombaert N, Wahis J, Van den Haute C, Holt MG, & Arckens L (2020). Astrocytes shape the plastic response of adult cortical neurons to vision loss. Glia, 68(10), 2102–2118. 10.1002/glia.23830 [PubMed: 32237182]

Herculano-Houzel S (2014). The glia/neuron ratio: How it varies uniformly across brain structures and species and what that means for brain physiology and evolution. Glia, 62(9), 1377–1391. 10.1002/glia.22683 [PubMed: 24807023]

Huang AY, Woo J, Sardar D, Lozzi B, Bosquez Huerta NA, Lin CJ, Felice D, Jain A, Paulucci-Holthauzen A, & Deneen B (2020). Region-specific transcriptional control of astrocyte function oversees local circuit activities. Neuron, 106(6), 992–1008 e1009. 10.1016/j.neuron.2020.03.025 [PubMed: 32320644]

Ji RR, Donnelly CR, & Nedergaard M (2019). Astrocytes in chronic pain and itch. Nature Reviews. Neuroscience, 20(11), 667–685. 10.1038/s41583-019-0218-1 [PubMed: 31537912]

Jonnalagadda D, Kihara Y, Rivera R, & Chun J (2021). S1P2-Galpha12 signaling controls astrocytic glutamate uptake and mitochondrial oxygen consumption. eNeuro, 8(4), ENEURO.0040-21.2021. 10.1523/ENEURO.0040-21.2021

Jung CG, Kim HJ, Miron VE, Cook S, Kennedy TE, Foster CA, Antel JP, & Soliven B (2007). Functional consequences of S1P receptor modulation in rat oligodendroglial lineage cells. Glia, 55(16), 1656–1667. 10.1002/glia.20576 [PubMed: 17876806]

Kajimoto T, Okada T, Yu H, Goparaju SK, Jahangeer S, & Nakamura S (2007). Involvement of sphingosine-1-phosphate in glutamate secretion in hippocampal neurons. Molecular and Cellular Biology, 27(9), 3429–3440. 10.1128/MCB.01465-06 [PubMed: 17325039]

Karunakaran I, & van Echten-Deckert G (2017). Sphingosine 1-phosphate - a double edged sword in the brain. Biochim Biophys Acta Biomembr, 1859(9 Pt B), 1573–1582. 10.1016/j.bbamem.2017.03.008 [PubMed: 28315304]

Khakh BS, & Sofroniew MV (2015). Diversity of astrocyte functions and phenotypes in neural circuits. Nature Neuroscience, 18(7), 942–952. 10.1038/nn.4043 [PubMed: 26108722]

Kim S, Bielawski J, Yang H, Kong Y, Zhou B, & Li J (2018). Functional antagonism of sphingosine-1-phosphate receptor 1 prevents cuprizone-induced demyelination. Glia, 66(3), 654–669. 10.1002/glia.23272 [PubMed: 29193293]

Kofuji P, & Araque A (2021). G-protein-coupled receptors in astrocyte-neuron communication. Neuroscience, 456, 71–84. 10.1016/j.neuroscience.2020.03.025 [PubMed: 32224231]

Kordula T, Rydel RE, Brigham EF, Horn F, Heinrich PC, & Travis J (1998). Oncostatin M and the interleukin-6 and soluble interleukin-6 receptor complex regulate alpha1-antichymotrypsin expression in human cortical astrocytes. The Journal of Biological Chemistry, 273(7), 4112–4118. 10.1074/jbc.273.7.4112 [PubMed: 9461605]

Lavialle M, Aumann G, Anlauf E, Prols F, Arpin M, & Derouiche A (2011). Structural plasticity of perisynaptic astrocyte processes involves ezrin and metabotropic glutamate receptors. Proceedings of the National Academy of Sciences of the United States of America, 108(31), 12915–12919. 10.1073/pnas.1100957108 [PubMed: 21753079]

Lee H, Deng J, Kujawski M, Yang C, Liu Y, Herrmann A, Kortylewski M, Horne D, Somlo G, Forman S, Jove R, & Yu H (2010). STAT3-induced S1PR1 expression is crucial for persistent STAT3 activation in tumors. Nature Medicine, 16(12), 1421–1428. 10.1038/nm.2250

Liang J, Nagahashi M, Kim EY, Harikumar KB, Yamada A, Huang WC, Hait NC, Allegood JC, Price MM, Avni D, Takabe K, Kordula T, Milstien S, & Spiegel S (2013). Sphingosine-1-phosphate links persistent STAT3 activation, chronic intestinal inflammation, and development of colitis-associated cancer. Cancer Cell, 23(1), 107–120. 10.1016/j.ccr.2012.11.013 [PubMed: 23273921]

Liddelow SA, Guttenplan KA, Clarke LE, Bennett FC, Bohlen CJ, Schirmer L, Bennett ML, Munch AE, Chung WS, Peterson TC, Wilton DK, Frouin A, Napier BA, Panicker N, Kumar M, Buckwalter MS, Rowitch DH, Dawson VL, Dawson TM … Barres BA (2017). Neurotoxic reactive astrocytes are induced by activated microglia. Nature, 541(7638), 481–487. 10.1038/nature21029 [PubMed: 28099414]

Lordkipanidze T, & Dunaevsky A (2005). Purkinje cell dendrites grow in alignment with Bergmann glia. Glia, 51(3), 229–234. 10.1002/glia.20200 [PubMed: 15800897]

Martin R, Bajo-Graneras R, Moratalla R, Perea G, & Araque A (2015). Circuit-specific signaling in astrocyte-neuron networks in basal ganglia pathways. Science, 349(6249), 730–734. 10.1126/science.aaa7945 [PubMed: 26273054]

Miller SJ, Philips T, Kim N, Dastgheyb R, Chen Z, Hsieh YC, Daigle JG, Datta M, Chew J, Vidensky S, Pham JT, Hughes EG, Robinson MB, Sattler R, Tomer R, Suk JS, Bergles DE, Haughey N, Pletnikov M, … Rothstein JD (2019). Molecularly defined cortical astroglia subpopulation modulates neurons via secretion of Norrin. Nature Neuroscience, 22(5), 741–752. 10.1038/s41593-019-0366-7 [PubMed: 30936556]

Morel L, Higashimori H, Tolman M, & Yang Y (2014). VGluT1+ neuronal glutamatergic signaling regulates postnatal developmental maturation of cortical protoplasmic astroglia. The Journal of Neuroscience, 34(33), 10950–10962. 10.1523/JNEUROSCI.1167-14.2014 [PubMed: 25122895]

Pan B, Guo Y, Wu HE, Park J, Trinh VN, Luo ZD, & Hogan QH (2016). Thrombospondin-4 divergently regulates voltage-gated Ca2+ channel subtypes in sensory neurons after nerve injury. Pain, 157(9), 2068–2080. 10.1097/j.pain.0000000000000612 [PubMed: 27168360]

Park J, Yu YP, Zhou CY, Li KW, Wang D, Chang E, Kim DS, Vo B, Zhang X, Gong N, Sharp K, Steward O, Vitko I, Perez-Reyes E, Eroglu C, Barres B, Zaucke F, Feng G, & Luo ZD (2016). Central mechanisms mediating Thrombospondin-4-induced pain states. The Journal of Biological Chemistry, 291(25), 13335–13348. 10.1074/jbc.M116.723478 [PubMed: 27129212]

Risher WC, Patel S, Kim IH, Uezu A, Bhagat S, Wilton DK, Pilaz LJ, Singh Alvarado J, Calhan OY, Silver DL, Stevens B, Calakos N, Soderling SH, & Eroglu C (2014). Astrocytes refine cortical connectivity at dendritic spines. eLife, 3, e04047. 10.7554/eLife.04047

Seddighi S, Varma VR, An Y, Varma S, Beason-Held LL, Tanaka T, Kitner-Triolo MH, Kraut MA, Davatzikos C, & Thambisetty M (2018). SPARCL1 accelerates symptom onset in Alzheimer's disease and influences brain structure and function during aging. Journal of Alzheimer's Disease, 61(1), 401–414. 10.3233/JAD-170557

Singh SK, & Spiegel S (2019). Sphingosine-1-phosphate signaling: A novel target for simultaneous adjuvant treatment of triple negative breast cancer and chemotherapy-induced neuropathic pain. In Press.

Singh SK, Stogsdill JA, Pulimood NS, Dingsdale H, Kim YH, Pilaz LJ, Kim IH, Manhaes AC, Rodrigues WS Jr., Pamukcu A, Enustun E, Ertuz Z, Scheiffele P, Soderling SH, Silver DL, Ji RR, Medina AE, & Eroglu C (2016). Astrocytes assemble Thalamocortical synapses by bridging NRX1alpha and NL1 via Hevin. Cell, 164(1–2), 183–196. 10.1016/j.cell.2015.11.034 [PubMed: 26771491]

Singh SK, Wilczynska KM, Grzybowski A, Yester J, Osrah B, Bryan L, Wright S, Griswold-Prenner I, & Kordula T (2011). The unique transcriptional activation domain of nuclear factor-I-X3 is critical to specifically induce marker gene expression in astrocytes. The Journal of Biological Chemistry, 286(9), 7315–7326. 10.1074/jbc.M110.152421 [PubMed: 21189253]

Spiegel S, & Milstien S (2011). The outs and the ins of sphingosine-1-phosphate in immunity. Nature Reviews. Immunology, 11(6), 403–415. 10.1038/nri2974

Stockstill K, Doyle TM, Yan X, Chen Z, Janes K, Little JW, Braden K, Lauro F, Giancotti LA, Harada CM, Yadav R, Xiao WH, Lionberger JM, Neumann WL, Bennett GJ, Weng HR, Spiegel S, & Salvemini D (2018). Dysregulation of sphingolipid metabolism contributes to bortezomib-induced neuropathic pain. The Journal of Experimental Medicine, 215(5), 1301–1313. 10.1084/jem.20170584 [PubMed: 29703731]

Stogsdill JA, & Eroglu C (2017). The interplay between neurons and glia in synapse development and plasticity. Current Opinion in Neurobiology, 42, 1–8. 10.1016/j.conb.2016.09.016 [PubMed: 27788368]

Stogsdill JA, Ramirez J, Liu D, Kim YH, Baldwin KT, Enustun E, Ejikeme T, Ji RR, & Eroglu C (2017). Astrocytic neuroligins control astrocyte morphogenesis and synaptogenesis. Nature, 551(7679), 192–197. 10.1038/nature24638 [PubMed: 29120426]

Terai K, Soga T, Takahashi M, Kamohara M, Ohno K, Yatsugi S, Okada M, & Yamaguchi T (2003). Edg-8 receptors are preferentially expressed in oligodendrocyte lineage cells of the rat CNS. Neuroscience, 116(4), 1053–1062. 10.1016/s0306-4522(02)00791-1 [PubMed: 12617946]

Toman RE, Payne SG, Watterson KR, Maceyka M, Lee NH, Milstien S, Bigbee JW, & Spiegel S (2004). Differential transactivation of sphingosine-1-phosphate receptors modulates NGF-induced neurite extension. The Journal of Cell Biology, 166(3), 381–392. 10.1083/jcb.200402016 [PubMed: 15289497]

Tsai HH, Li H, Fuentealba LC, Molofsky AV, Taveira-Marques R, Zhuang H, Tenney A, Murnen AT, Fancy SP, Merkle F, Kessaris N, Alvarez-Buylla A, Richardson WD, & Rowitch DH (2012). Regional astrocyte allocation regulates CNS synaptogenesis and repair. Science, 337(6092), 358–362. 10.1126/science.1222381 [PubMed: 22745251]

Wang G, & Bieberich E (2018). Sphingolipids in neurodegeneration (with focus on ceramide and S1P). Advances in Biological Regulation, 70, 51–64. 10.1016/j.jbior.2018.09.013 [PubMed: 30287225]

Wilczynska KM, Singh SK, Adams B, Bryan L, Rao RR, Valerie K, Wright S, Griswold-Prenner I, & Kordula T (2009). Nuclear factor I isoforms regulate gene expression during the differentiation of

human neural progenitors to astrocytes. Stem Cells, 27(5), 1173–1181. 10.1002/stem.35 [PubMed: 19418463]

Yang L, Qi Y, & Yang Y (2015). Astrocytes control food intake by inhibiting AGRP neuron activity via adenosine A1 receptors. Cell Reports, 11(5), 798–807. 10.1016/j.celrep.2015.04.002 [PubMed: 25921535]

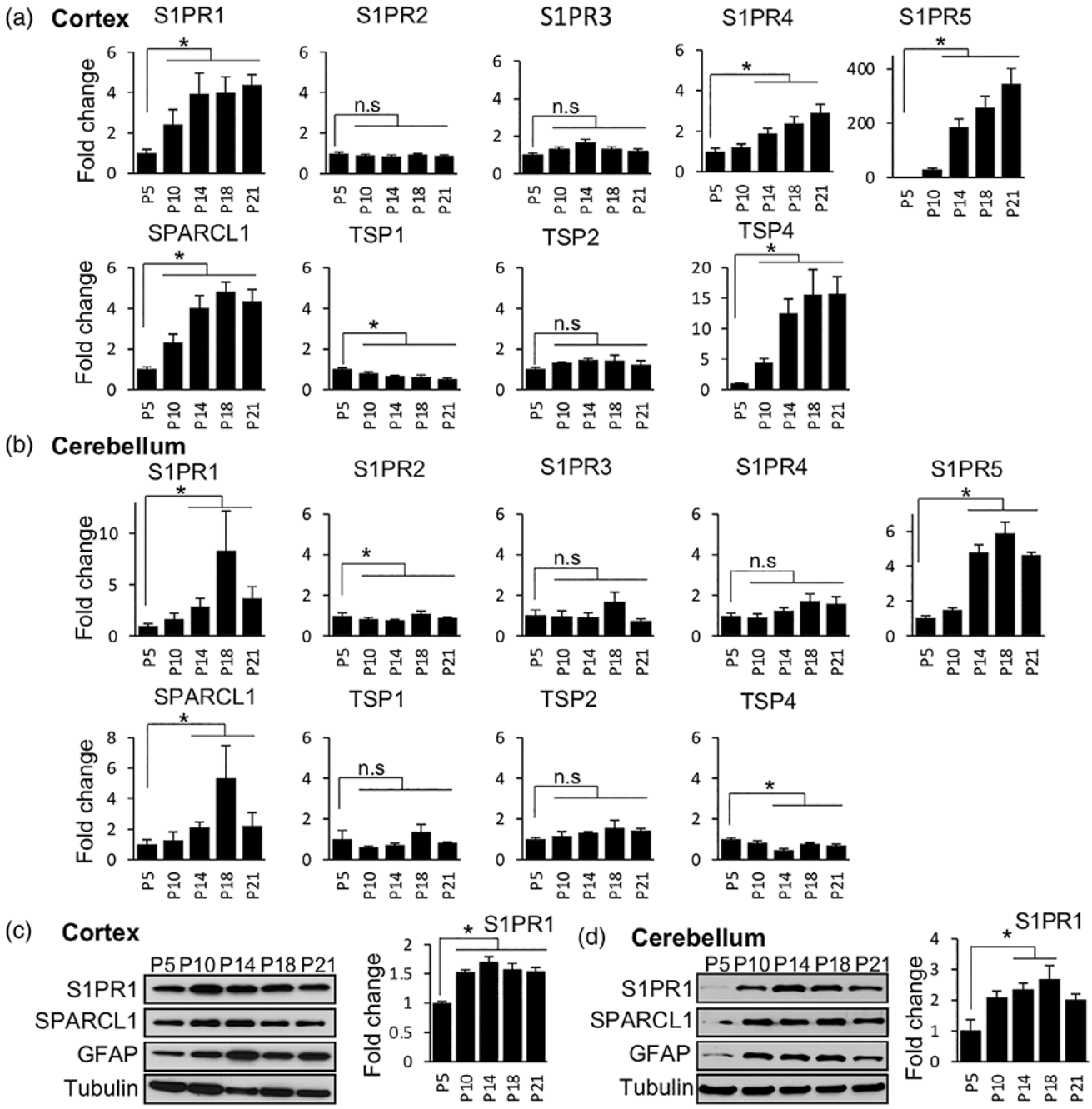


**FIGURE 1.**

Dynamic expression of S1PRs and astrocyte-secreted synaptogenic factors during mouse brain development. (a, b) Expression of S1PR1-5 and major synaptogenic factors determined by qPCR in the cortices (a) and cerebella (b) of mouse brain at the indicated postnatal age. Data were normalized to 18S RNA and expressed as fold change relative to the expression at P5. $n \geq 5$ independent measurements from three brains at each time point. Data are mean ± SD, $*p < .05$, determined by one way ANOVA followed by Tukey's multiple comparison test. (c, d) Protein levels of S1PR1, SPARCL1, and GFAP in the cortices (c) and cerebella

(d) at the indicated postnatal age determined by western blotting. Tubulin was used as a loading control. S1PR1 blots were quantified relative to tubulin by densitometry and expressed as fold change relative to P5 (right panels)

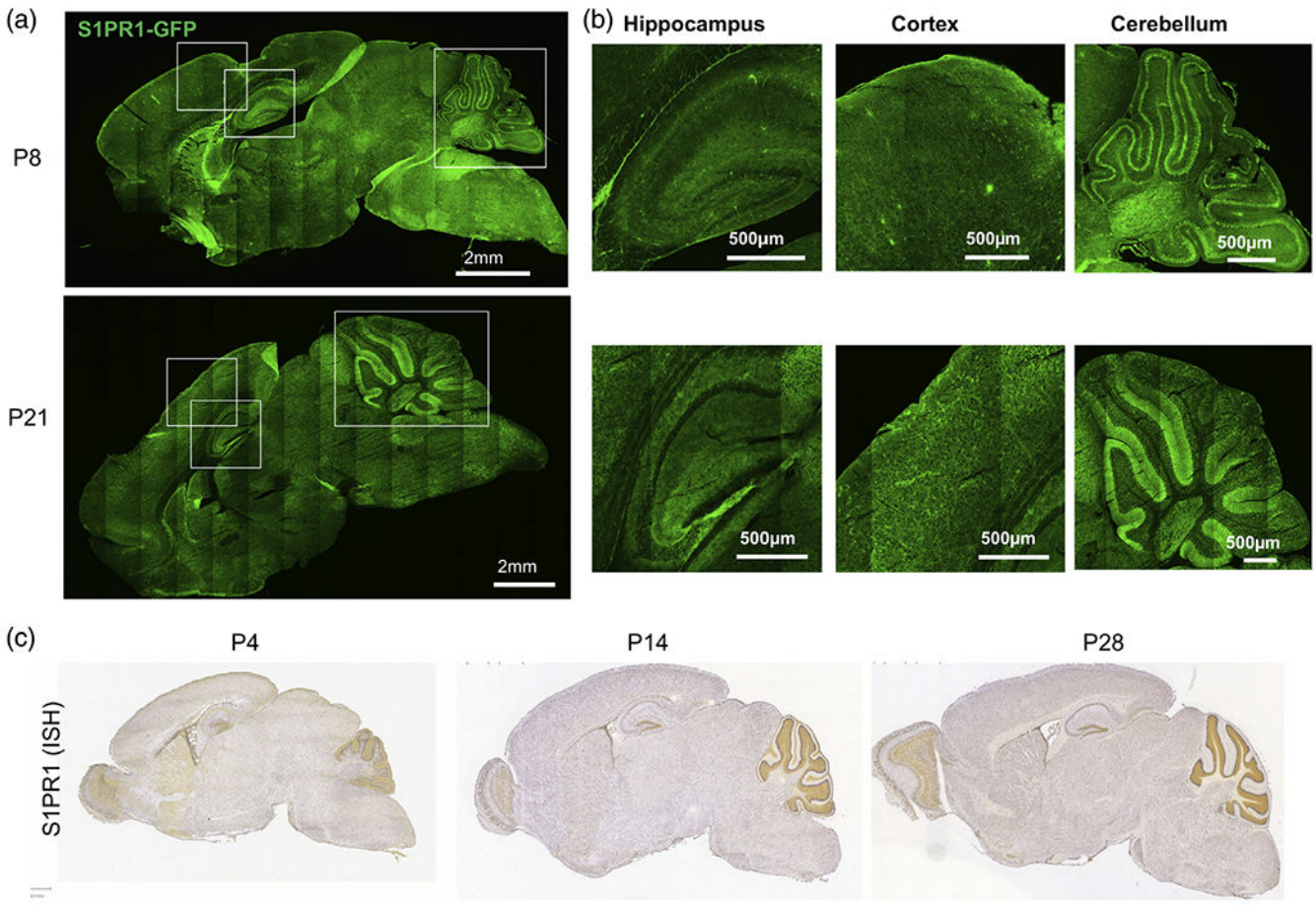


**FIGURE 2.**

Widespread expression of S1PR1 in the brain. (a) eGFP fluorescence of sagittal sections of S1PR1-eGFP mouse brains at P8 (top) and P21 (bottom). (b) Enlarged images of the indicated cortical, hippocampal and cerebellar regions from panel (a). (c) In situ hybridization (ISH) data for S1PR1 (Allen brain atlas) at the indicated time points of mouse brain development

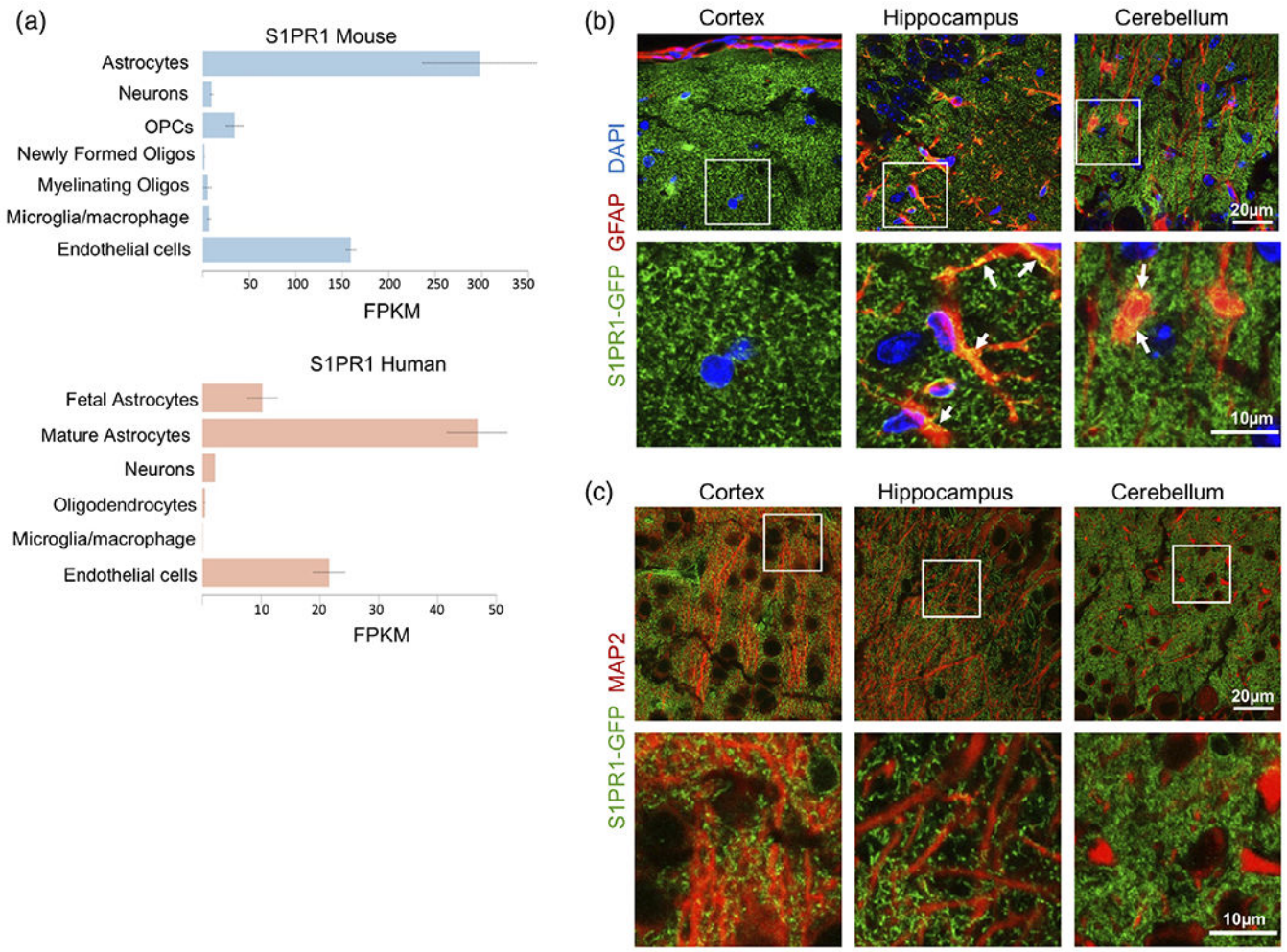


**FIGURE 3.**

S1PR1 is expressed in mouse and human astrocytes. (a) Expression of S1PR1 in the various brain cell types (www.brainrnaseq.org). FPKM: fragments per kilobase of transcript per million mapped reads. (b, c) Confocal images of S1PR1-eGFP (green), astrocytic marker GFAP (red) (b) or neuronal dendrite marker MAP2 (red) (c) in cortical, hippocampal and cerebellar regions from P21 S1PR1-eGFP mice

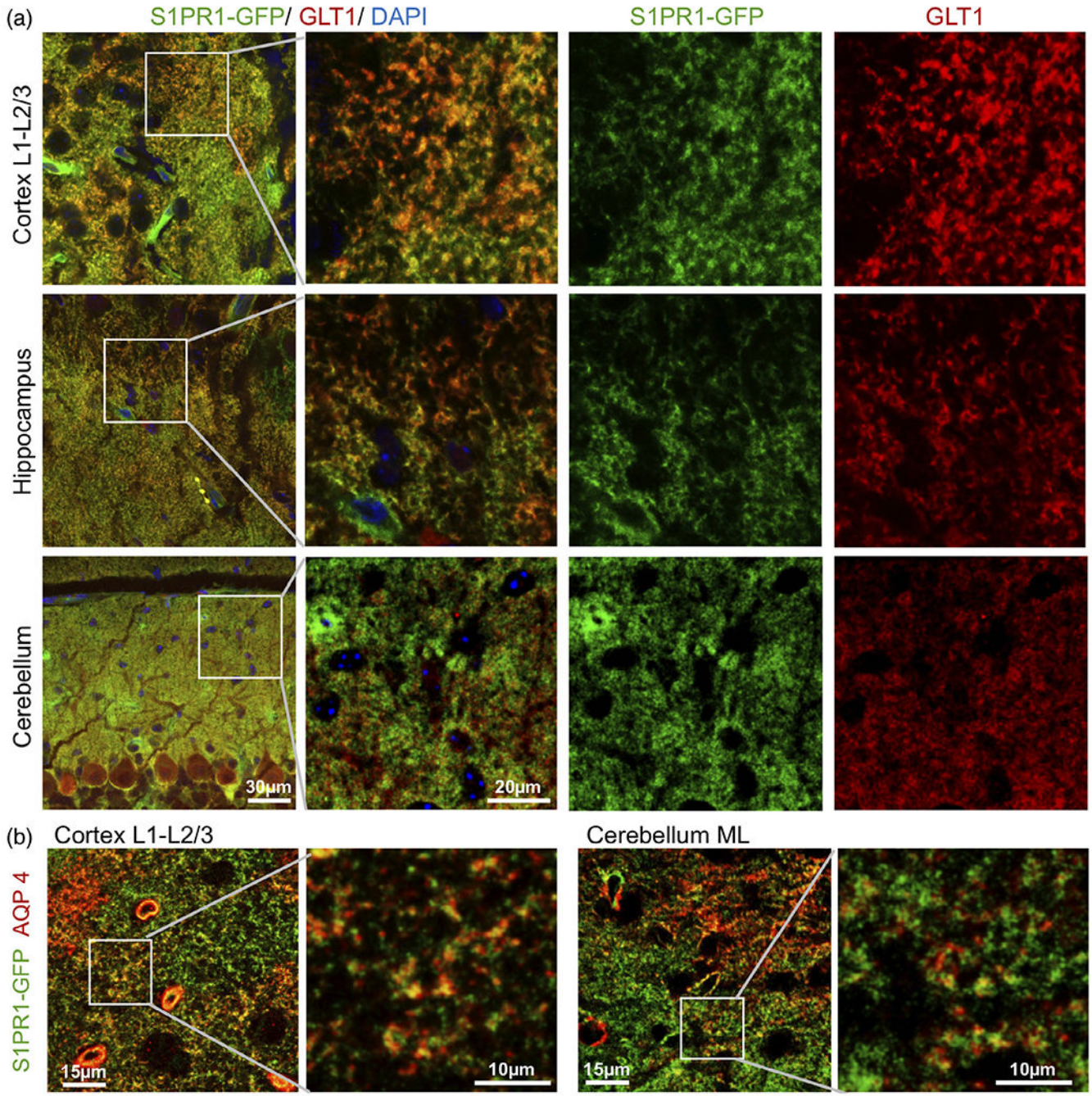


**FIGURE 4.**

S1PR1 is highly expressed on perisynaptic astrocyte processes. (a) Confocal images of S1PR1-eGFP (green) in cortical layer L1-L2/3, hippocampus, and cerebellar molecular layer from P21 S1PR1-eGFP mice immunostained for (a) astrocytic glutamate transporter GLT1 (red) or (b) astrocyte aquaporin 4 (AQP4) (red) as indicated. Enlarged boxed areas are shown (lower panels)

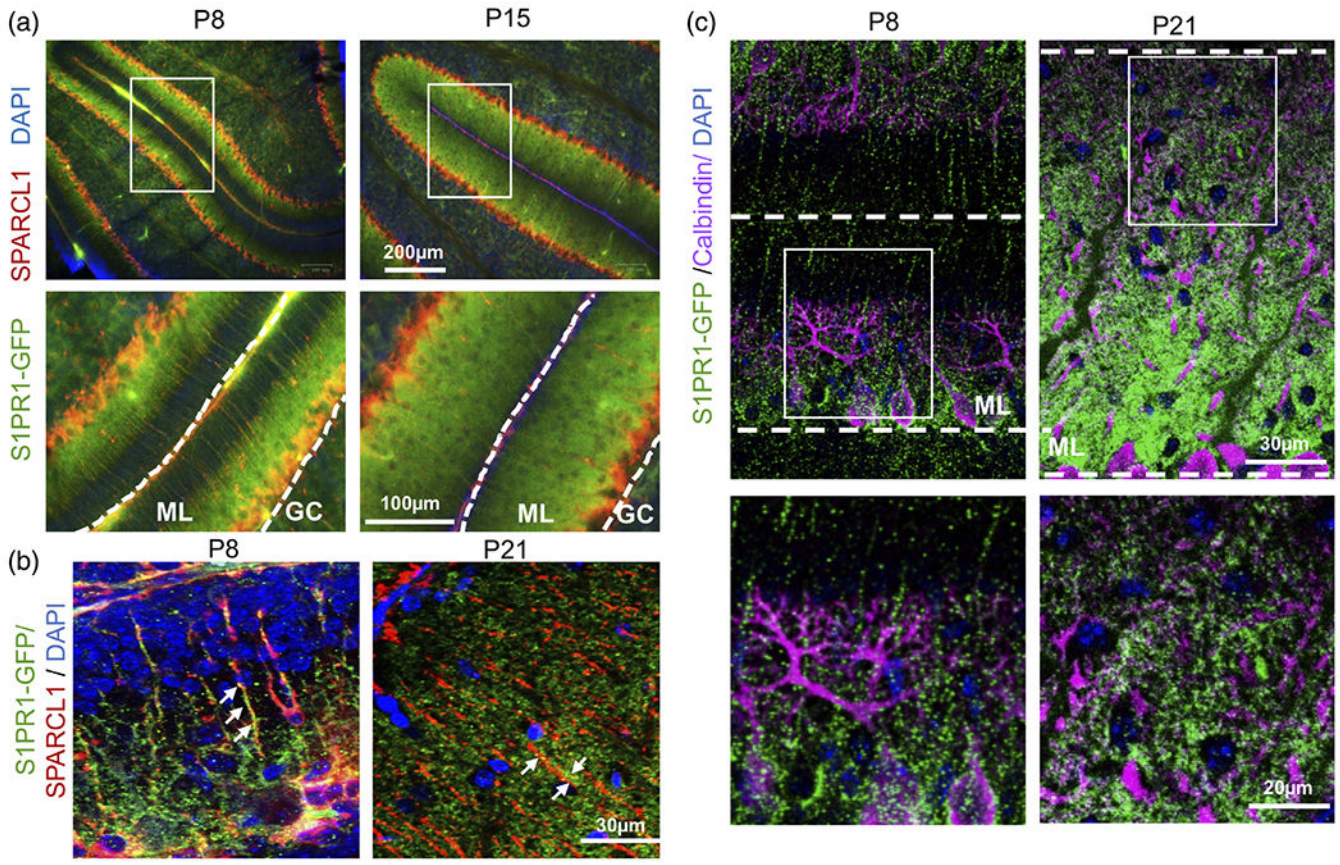


**FIGURE 5.**

Developmental expression of S1PR1 by Bregman glia. (a–c) Confocal images of S1PR1-eGFP (green) of cerebellar sections at postnatal days P8, P15, and P21 from S1PR1-eGFP transgenic mice immunostained for SPARCL1 (red) or calbindin (magenta). Enlarged boxed areas are shown. GC, granular layer; ML, molecular layer

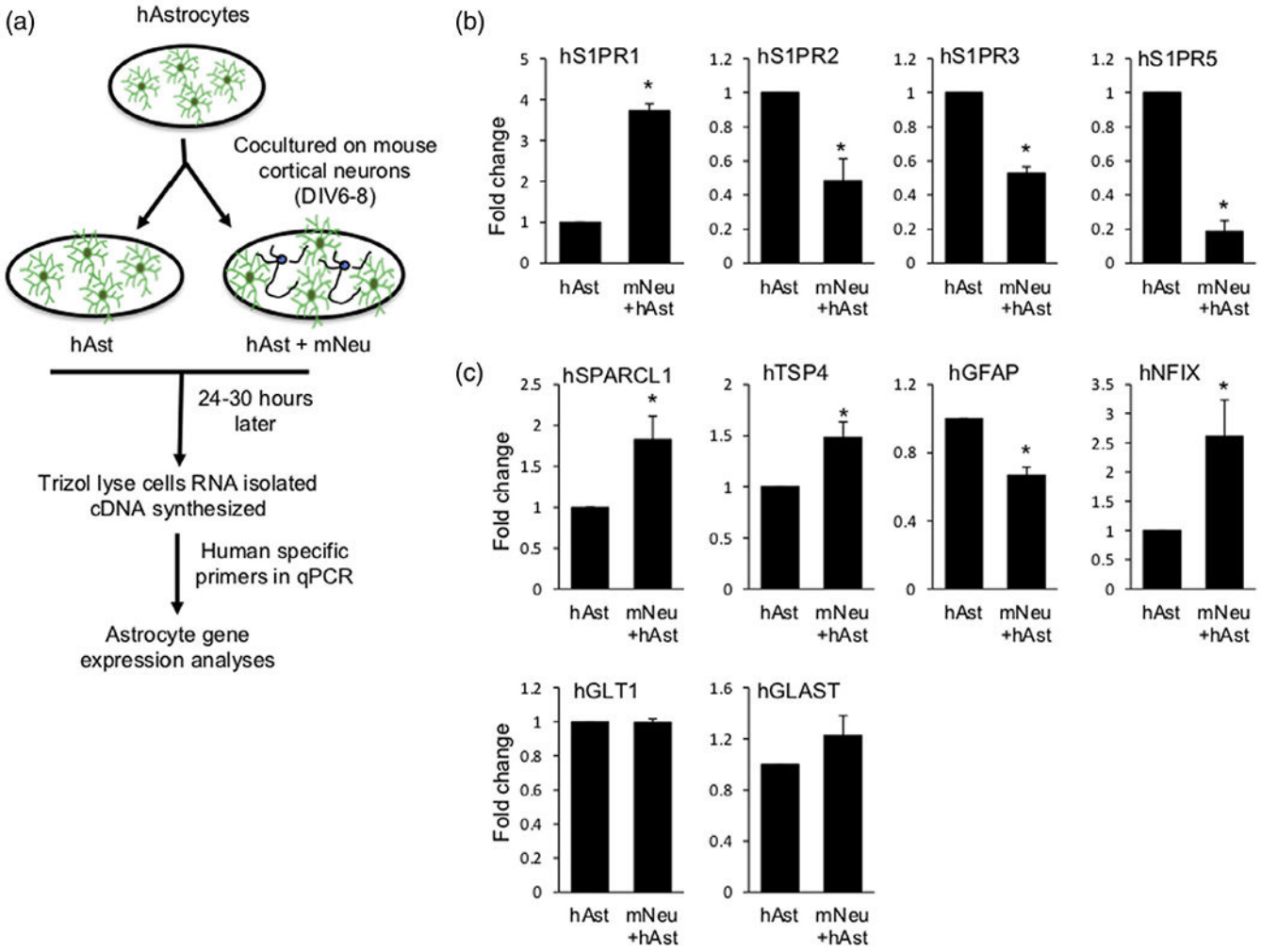


**FIGURE 6.**

Neuronal contact stimulates S1PR1 expression in astrocytes. (a) Diagram of the mouse cortical neuron and human astrocyte coculture system. (b, c) qPCR analyses of expression of astrocytic S1PRs (b) and synaptogenic and maturation markers (c) in human astrocytes cultured alone or co-cultured with mouse cortical neurons. Data were normalized to GAPDH and presented as fold expression compared to astrocytes alone. $n = 3$ independent primary cell preparation experiments. Data are mean ± SEM, $*p < .05$, two tailed Student's $t$-test. For NFIX, $*p < .05$, one tailed Student's $t$-test

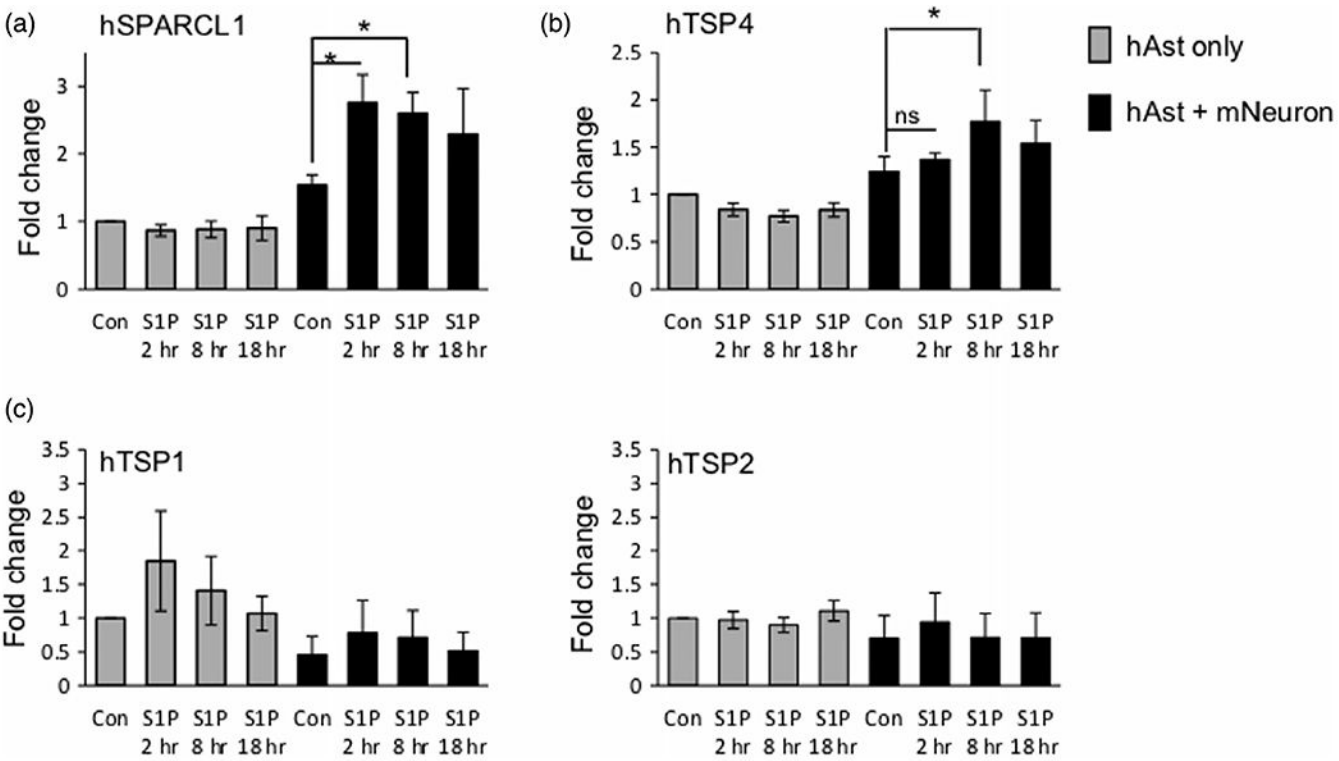


**FIGURE 7.**

S1P specifically upregulates expression of synaptogenic factors in astrocytes cocultured with neurons. (a–c) Human astrocytes were cultured in the absence or presence of mouse cortical neurons and stimulated without or with 100 nM S1P. Expression of astrocyte synaptogenic factors was determined by qPCR and normalized to GAPDH presented as fold expression compared to untreated astrocytes alone. $n = 3$ independent culture experiments. Data are expressed as means ± SEM. $*p < .05$, one way ANOVA followed by Sidak's multiple comparison test

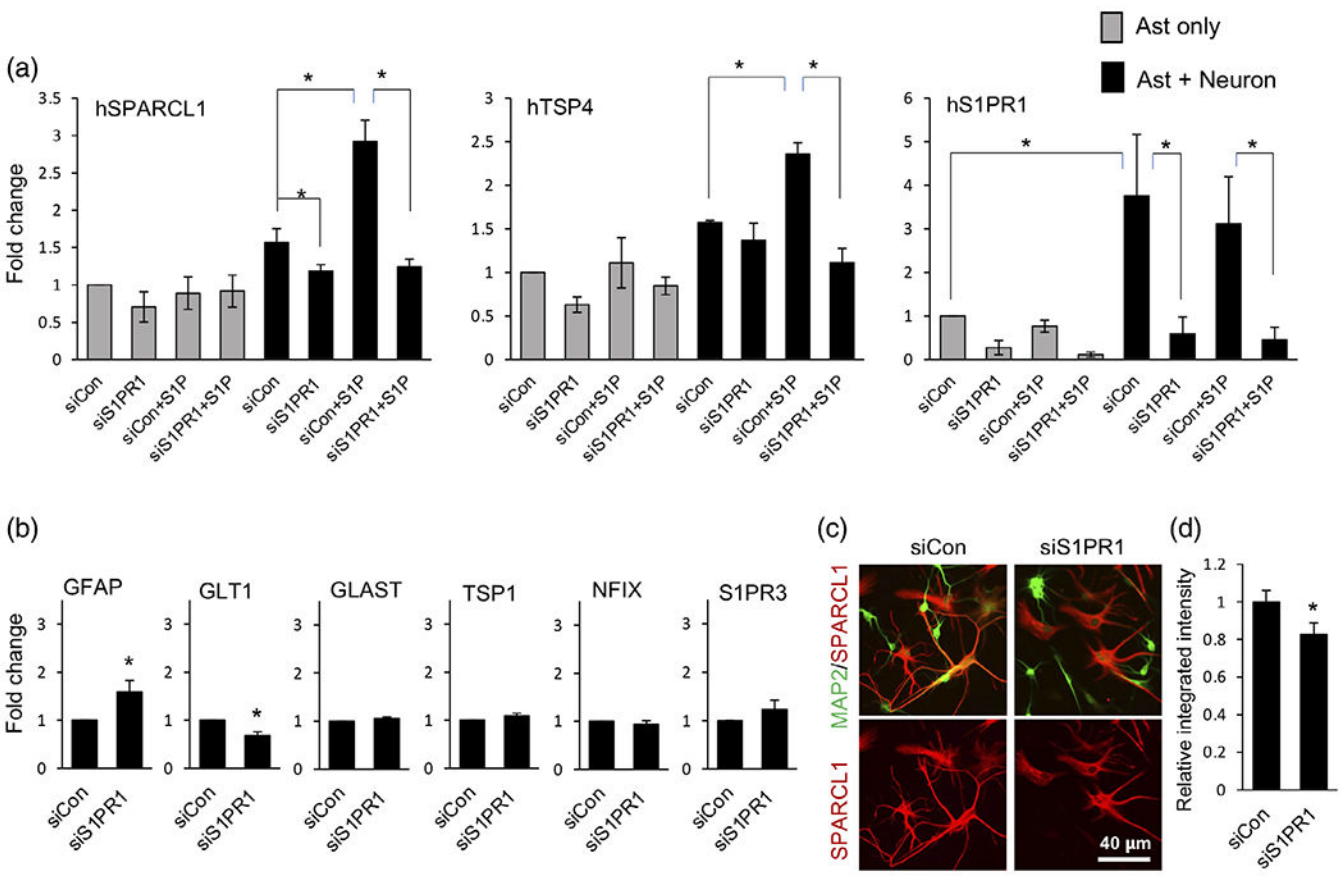


**FIGURE 8.**

Neuronal contact induces astrocyte expression of SPARCL1 and TSP4 via astrocytic S1PR1. Human astrocytes were transfected with either siRNA targeting S1PR1 (siS1PR1) or control siRNA (siCon), then cultured in the presence (a) or absence (b) of mouse neurons and stimulated without or with 100 nM S1P. Expression of synaptogenic factors (a) and maturation markers (b) was determined by qPCR and normalized to GAPDH presented as fold expression compared to siCon. Data are expressed as means ± SEM. $n = 3$ independent culture experiments, $*p < .05$, one way ANOVA followed by Sidak's multiple comparison test (a) or 2-tailed $t$-test (b). (c) Representative image of SPARCL1 (red) immunostaining in astrocytes cocultured with neurons stained for MAP2 (Green). Right panel shows quantification of SPARCL1 fluorescence (red) intensity plotted as relative integrated density per area compared to siCon condition. Data are expressed as means ± SEM, $n = 55–60$ images per condition of nine independent cultures from three separate primary cell preparations, $*p < .05$, two tailed Student's $t$-test

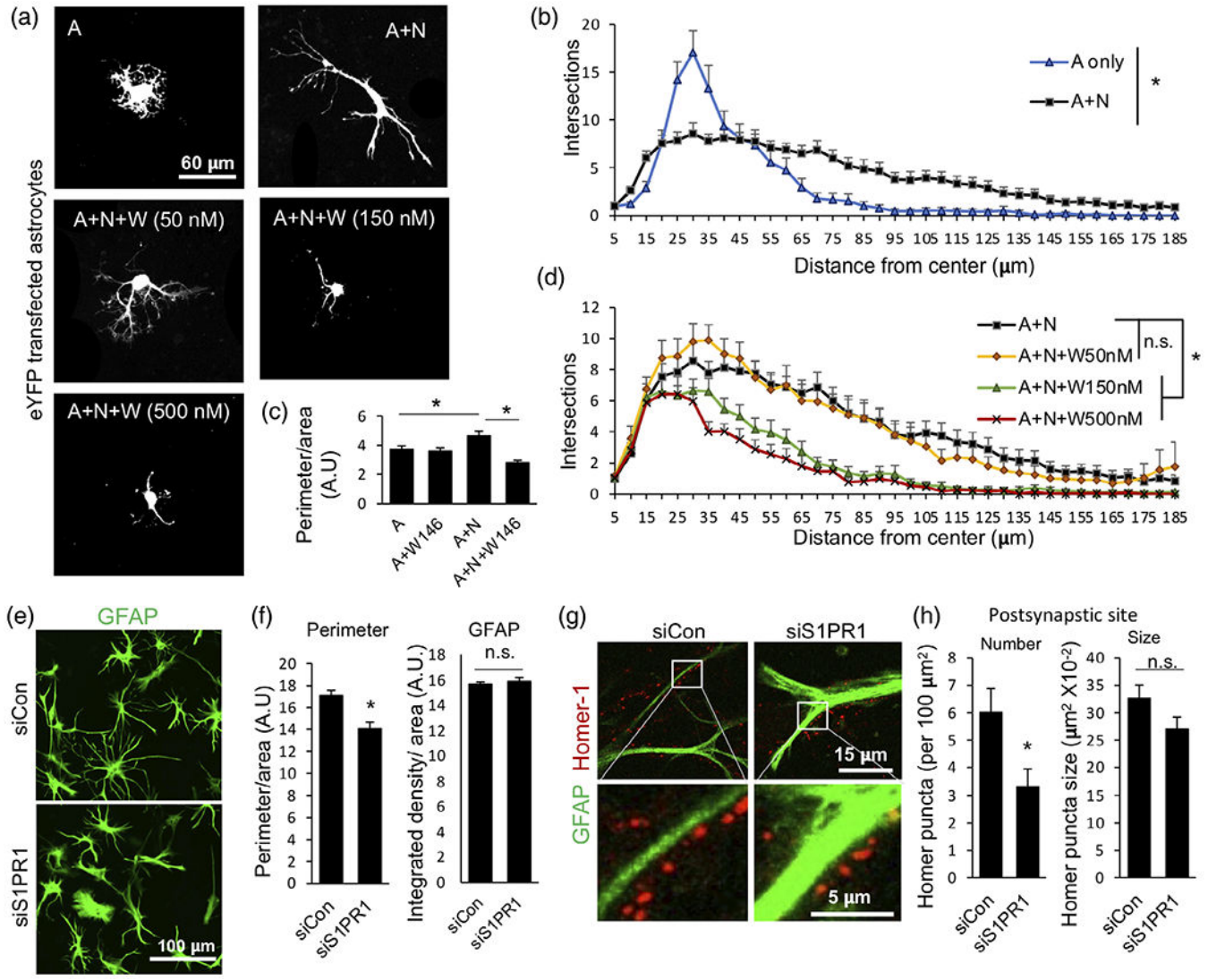


**FIGURE 9.**

S1PR1 regulates neuron-induced astrocyte morphological complexity and postsynapse association. (a) Representative images of eYFP transfected astrocytes cultured alone or with neurons in the presence or absence of 50, 150, or 500 nM W146. (b, d) Quantitation of astrocyte morphological complexity by Sholl analysis. Data is presented as numbers of total intersections at the indicated distance from the center of the cell body. $n = 34–42$ images per condition from six independent cultures from two primary cell preparations. Similar results were obtained in another 3rd biological replicate with 150 nM W146. Data are mean ± SEM; *$p < .05$, one way ANOVA followed by Kruskal-Wallis test for the entire curves. (c) Quantitative analyses of perimeters of eYFP transfected astrocytes. Data are expressed as perimeter of eYFP filled area. $n > 20$ images per condition from three independent cultures; data are mean ± SEM; *$p < .05$, one way ANOVA followed by Sidak's multiple comparison test. (e) Representative image of immunostained GFAP (green) in siCon or siS1PR1treated astrocytes cocultured with neurons. Quantitative analyses of images from (e) used to determine perimeter of astrocytes (f). Data are expressed as perimeter per GFAP

filled area (left panel) or GFAP intensity (right panel). $n$ = 38–40 images per condition from six independent cultures from two separate primary cell preparations. Similar results were obtained in another 3rd biological replicate experiment. Data are mean ± SEM; *$p$ < .05, two tailed Student's $t$-test. (g) Representative images of synapse (homer-1, red) association with siCon or siS1PR1 transfected astrocytes (GFAP, green) in cocultures. (h) Quantification of homer-1 puncta association with astrocytes. Data are numbers per 100 μm$^2$ area of GFAP positive astrocytes (left) or size of homer-1 puncta (right). $n$ = 30–36 images per condition from six independent cultures from two separate primary cell preparations. Data are mean ± SEM; *$p$ < .05, two tailed Student's $t$-test